

THE FLORIDA STATE UNIVERSITY
COLLEGE OF ARTS AND SCIENCES

DISSIPATION PROCESSES IN THE
TONGUE OF THE OCEAN

By

JAMES A. HOOPER V

A Thesis submitted to the
Department of Earth, Ocean, and Atmospheric Sciences
in partial fulfillment of the
requirements for the degree of
Master of Science

Degree Awarded:
Spring Semester, 2011

The members of the committee approve the Thesis of James Hooper defended on March 31, 2011.

William Dewar
Professor Directing Thesis

Louis St. Laurent
Committee Member

Carol Anne Clayson
Committee Member

Joel Kostka
Committee Member

Approved:

Lynn Dudley, Chair, Department of Earth, Ocean,
and Atmospheric Sciences

Joseph Travis, Dean, College of Arts and Sciences

The Graduate School has verified and approved the above-named committee

ACKNOWLEDGEMENTS

I would like to thank my principle advisor, Dr. Louis St. Laurent, for his guidance and support throughout my research process. Louis provided me with a rich experience at The Florida State University giving me opportunities to travel and participate in oceanographic research cruises. I also owe Dr. William K. Dewar great deal of gratitude for taking over as my major professor during my final year of study. Dr. Dewar was instrumental in helping with the final editing of my paper and was an invaluable resource for any questions that arose along the process. In addition, I would also like to thank my other committee members for their support, Dr. Joel Kostka and Dr. Carol Anne Clayson.

I would also like to thank Doug Nowacek and Elliot Hazen for their help with the biological data. I also would like to thank Austin Todd for his help in the initial editing of my paper. I would also like to thank Bryan Rahter and Nicolas Weinders for their various perspectives on my work.

My experience at FSU was greatly enhanced thanks to a wonderful group of friends. I would also like to thank my family: my parents, Jim and Anne; my sister Sarah; and my brother and his family; Jason, Jennifer, and their son Jake, whose love and encouragement have kept my life in focus and my goals in sight.

TABLE OF CONTENTS

List of Figures.....	v
Abstract.....	vii
INTRODUCTION.....	1
BACKGROUND.....	5
QUANTIFYING PARAMETERS.....	7
1.1 Dissipation.....	7
1.2 Shear.....	7
1.3 Volume Backscattering Strength.....	8
INSTRUMENTATION.....	9
1.4 Deep Microstructure Profiler (DMP).....	9
1.5 Hydrographic Doppler Sonar System (HDSS).....	10
1.6 Simrad EK60 Echosounder.....	11
1.7 Data.....	11
OBSERVATIONS.....	12
1.8 Clover Survey Results.....	13
1.9 Clover Survey Discussion.....	18
1.10 Inter-Site Comparison.....	29
CONCLUSION.....	33
REFERENCES.....	35
BIOGRAPHICAL SKETCH.....	38

LIST OF FIGURES

1. Topography with cruise stations and nominal cruise tracks located in the Tongue of the Ocean. The two center stations (slightly offset for visibility) of each Clover are shown in green, with the apex station of each in red. The inset shows a close-up of the Clover 4 survey..... 2

2. Plot of clovers 2, 4, and 5 conducted during the DVM comparing the dissipation rates to the volume backscattering strength with the potential density contours in the background. The profile to the left is the dissipation profile with the acoustic profile to the right in each pair of profiles. The data is estimated over 50 m depth intervals with the bold vertical line representing the mean bin values and the white area the 95% confidence intervals. A logarithmic axis is used for the dissipation data plotted about a reference level of $\varepsilon = 1 \times 10^{-10} \text{ W kg}^{-1}$, corresponding to the background dissipation level. The acoustic data is plotted with a reference level of -90 db.... 14

3. Plot of clovers 6, 7, and 8 conducted post-DVM comparing the dissipation rates to the volume backscattering strength with the potential density contours in the background. The profile to the left is the dissipation profile with the acoustic profile to the right in each pair of profiles. The data is estimated over 50 m depth intervals with the bold vertical line representing the mean bin values and the white area the 95% confidence intervals. A logarithmic axis is used for the dissipation data plotted about a reference level of $\varepsilon = 1 \times 10^{-10} \text{ W kg}^{-1}$, corresponding to the background dissipation level. The acoustic data is plotted with a reference level of -90 db..... 15

4. Station 7 from clover 4 plotted on top of the volume backscattering strength time series. The slanted bold line represents the estimated location of the profile through the water column with time..... 16

5. Station 2 from clover 2 plotted on top of the volume backscattering strength time series. The slanted bold line represents the estimated location of the profile through the water column with time..... 17

6. Plot of the Clover 2 survey comparing the dissipation profiles plotted on top of the zonal shear. For reference the deep scattering

layer (DSL) resides approximately between 400 to 600 m.....	19
7. Plot of the Clover 4 survey comparing the dissipation profiles plotted on top of the zonal shear. For reference the deep scattering layer (DSL) resides approximately between 400 to 600 m.....	20
8. Plot of the Clover 8 survey comparing the dissipation profiles plotted on top of the meridional shear. For reference the deep scattering layer (DSL) resides approximately between 400 to 600 m.....	21
9. Plot of the Clover 7 survey comparing the dissipation profiles plotted on top of the zonal shear. For reference the deep scattering layer (DSL) resides approximately between 400 to 600 m.....	22
10. Gradient Richardson number (Ri) for Clover 2. The vertical blue line represents the critical Ri number, $Ri < 0.25$	25
11. Gradient Richardson number (Ri) for Clover 8. The vertical blue line represents the critical Ri number, $Ri < 0.25$	26
12. Correlation coefficients between dissipation rates and volume backscattering strength representing profiles below 300 m to eliminate surface signals. The horizontal bars with each dot represents the 95% confidence interval. The blue dotted line at 0.5 represents moderate or better correlations.....	27
13. Correlation coefficients between epsilon and zonal (black) and meridional (red) shear representing profiles below 300 m to eliminate surface signals. The horizontal bars with each dot represents the 95% confidence interval. The blue dotted line at 0.5 represents moderate or better correlations.....	28
14. Site map of the TOTO and NATRE locations.....	30
15. Ensemble average profiles of turbulent dissipation rate estimated from microstructure measurements at two different deep ocean sites. Depth bins of 50 m were used in calculations of the 95% confidence interval (colored bands) and mean (bold vertical lines inside each band).....	31

ABSTRACT

The Tongue of the Ocean (TOTO) region located within the Bahamas archipelago is a relatively under-studied region in terms of both its biological and physical oceanographic characteristics. This region is comprised of a deep trough along with steep boundaries that are commonly associated with elevated turbulent dissipation rates, ϵ , when impacted by currents and internal waves. A prey-field mapping cruise took place in the fall between 9/15/2008 and 10/01/2008, consisting of a series of transects and “clovers” to study the spatial and temporal variability. The region is characterized by a deep scattering layer (DSL), which is preyed on by nekton that serves as the food for beaked whale and other whale species. This study marks the first of its kind where concurrent measurements of acoustic backscatter and turbulence have been conducted for a nekton scattering layer well below the euphotic zone. In this novel study, turbulence data collected from a deep microstructure profiler are compared to biological and shear data collected by a 38 kHz Simrad EK 60 echosounder and a hydrographic Doppler sonar system, respectively. From these measurements, the primary processes responsible for the turbulent production in the TOTO region are assessed. The DSL around 500 m and a surface scattering layer (SSL) are investigated for raised ϵ values. Strong correlation between turbulence levels and scattering intensity of prey is generally found in the SSL with dissipation levels as large as $\sim 10^{-7} \text{ W kg}^{-1}$, three orders of magnitude above background levels. In the deep scattering layer, however, the correlations are relatively weak, but exhibit dissipation levels $\sim 10^{-8} \text{ W kg}^{-1}$. The absence of turbulence bursts of $O(10^{-5} \text{ W kg}^{-1})$ proposed to occur within dense biomass aggregations suggests biologically generated turbulence is not efficient by the marine biosphere.

Areas of elevated turbulence have many implications from sustaining the abyssal stratification to transporting of nutrients and gases to and from the surface. We

present an examination of the TOTO mixing levels with those from a typical open ocean site.

INTRODUCTION

The Bahamas archipelago (24°15'N, 76°W) is located off the southeast coast of Florida and to the northeast of Cuba (Figure 1). The Atlantic basin extends within the archipelago forming a deep-sea trough known as the Tongue of the Ocean. The region consists of predominantly easterly winds and the oceanic flow is generally to the northwest. This trough, along with scattered seamounts in the region, makes the TOTO a complex topographic region. The TOTO is a sheltered region protected by Andros Island to the west, the Exuma Cays to the east and the Grand Bahamas Banks to the south. The TOTO region ranges from 1500 to 3600 m deep, and is 32 to 64 km wide and 160 km long (Schwab *et al.*, 1989). This region is also home to several species of cetaceans, specifically Cuvier's and Blainville's beaked whales (MacLeod *et al.*, 2004), that use the sheltered waters for foraging. Mann and Jarvis (2004) observed what might possibly be sounds by deep-sea fishes between 500-700 m depth, most likely a biomass layer used in foraging, using the AUTEK range hydrophones in the TOTO region. However, the TOTO region is poorly studied in terms of both its biological and physical characteristics.

During September 2008 a joint survey between ocean mixing and whale prey-fields was conducted in the Tongue of the Ocean within the Bahamas Islands. This study used three different observation systems: a lowered deep microstructure profiler, a 38 kHz Simrad EK60 echosounder, and a 50 kHz HDSS mounted to the hull of the *R/V Roger Revelle*. The deep microstructure profiler (DMP) yields vertical profiles of dissipation rates. The echosounder indicates the location of biomass layers in the water column through enhanced levels of

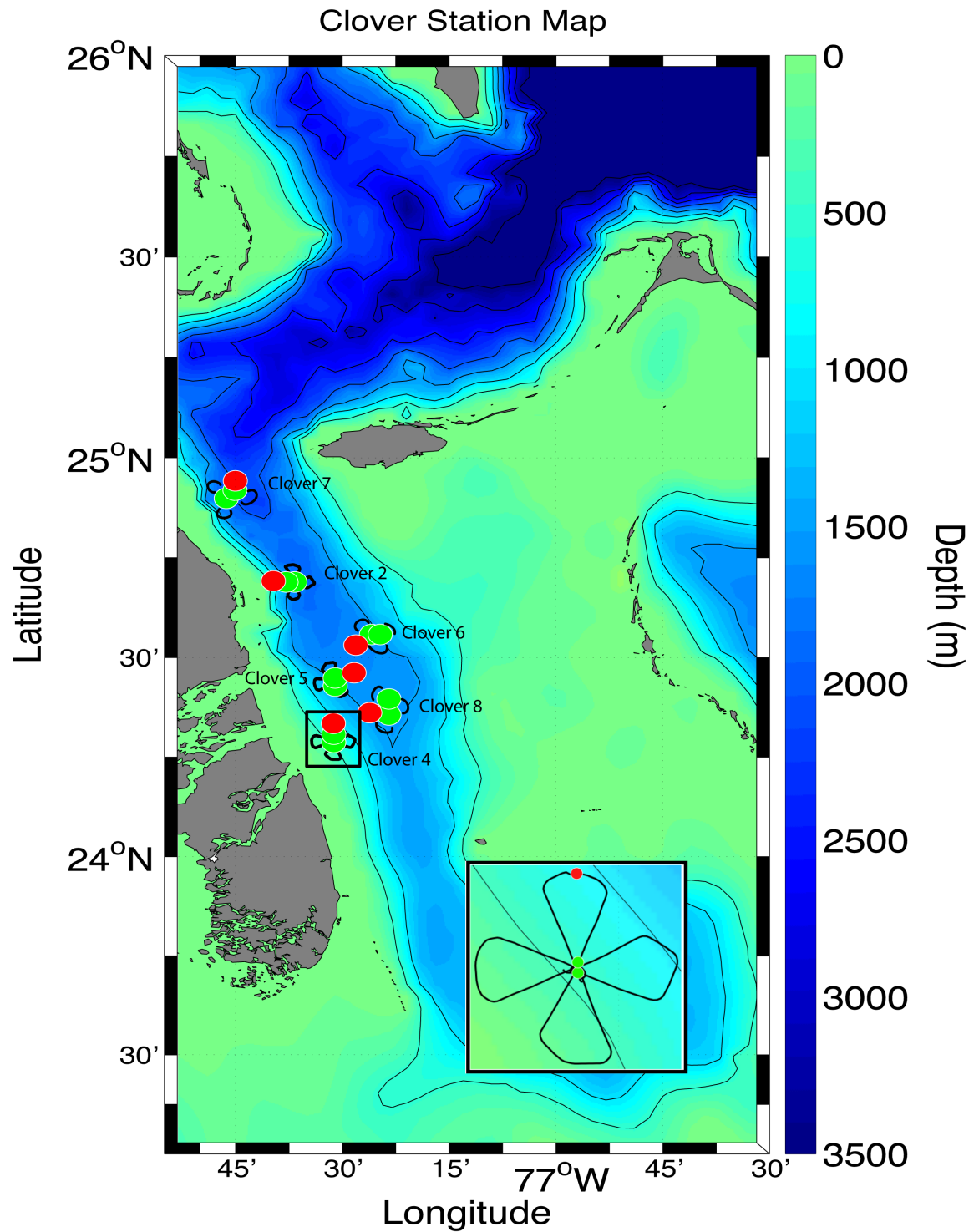


Figure 1. Topography with cruise stations and nominal cruise tracks located in the Tongue of the Ocean. The two center stations (slightly offset for visibility) of each Clover are shown in green, with the apex station of each in red. The inset shows a close-up of the Clover 4 survey.

acoustic backscatter. Finally, the HDSS provides velocities to 1000-m depth, which may be used to estimate shear.

These co-located measurements were used in complementary ways to determine the processes responsible for turbulence generation in the TOTO region. While previous studies (e.g. Kunze *et al.*, 2009; Gregg and Horne, 2009) have used co-located measurements of acoustic backscatter and microstructure profiles to measure biologically generated turbulence at the surface, this study differs in that the turbulent structure of the marine layers is obtained several hundred meters below the surface. This aggregation of biomass located in the deep ocean is known as the deep scattering layer. The deep scattering layer (DSL) is a dense permanent biomass layer found within the aphotic zone (often below 400 m), with a vertical thickness of 200-300 m and a horizontal spatial scale of thousands of meters. DSL's are found in nearly all the oceans (Brekhovskikh, L. M. and Y. P. Lysanov, 2003). There is also a more mobile marine layer that migrates from the DSL to the surface. This process is referred to as a diel vertical migration. Most often, a diel vertical migration (DVM) consists of marine animals ascending from the deep ocean to the surface at dusk, developing a surface scattering layer (SSL), followed by a return trip to the deep ocean at dawn (Hays *et al.*, 2003, Hays *et al.*, 2010). It is commonly believed that the DVM is a predatory evasion response, allowing these species to feed at the surface under the cover of dark at night before returning to the protection of the aphotic deep ocean during the day. Given this behavior, it is possible that the DVM could play an important role in the transport of gasses and nutrients to and from the surface.

Thus, the objectives of this study were to determine the relative inputs of the biology in the DSL, its associated DVM and the velocity shear to the turbulent dissipation rates observed in the TOTO region. In addition, this study addresses the Rothschild-Osborn hypothesis that the turbulent dissipation rates produced by the velocity shear may influence the position of the zooplankton in the water

column (Rothschild and Osborn, 1988). The clover survey was not designed to test the Rothschild-Osborn hypothesis, however we examine if the same effects are true for the DSL. Furthermore, the mixing levels of the enclosed TOTO region will be compared to the mixing levels of an open ocean region, the North Atlantic.

BACKGROUND

The generation of oceanic turbulence is dependent on the spatial and temporal distribution of the physical, topographic and biological features. Traditionally turbulence studies have focused on observations in the presence of strong currents or internal tides interacting with rift valleys, canyons, mid-ocean ridges, and open ocean seamounts (Lueck and Mudge, 1997, Polzin *et al.*, 1997, Ledwell *et al.*, 2000, St. Laurent and Thurnherr, 2007). The purpose of which has been to understand the energy sources responsible for sustaining the thermocline. Wunch and Ferrari (2004) argued that the turbulence production caused by tidal interactions with complex topography and by the winds were sufficient to account for the energetic requirements of mixing.

However, large scale mixing experiments involving both chemical tracers as well as vertical microstructure profiler measurements have observed that the average open-ocean mixing value, away from complex topography, is one magnitude smaller, $10^{-5} \text{ m}^2 \text{ s}^{-1}$ (Ledwell *et al.*, 1993, Toole *et al.*, 1994) than Munk's canonical value, $10^{-4} \text{ m}^2 \text{ s}^{-1}$ (Munk, 1966). This suggests that turbulence production only occurs in the presence of complex topography or other sources of turbulence production may contribute to maintain ocean stratification.

The study of biologically generated turbulence has become an increasing interest in the study of ocean turbulence. Dewar *et al.* (2006) question the closed nature of the energy budget and estimated the energy input of the biosphere into subsurface mechanical energy. Starting from the total energy produced by phytoplankton, the remainder of the energy yielded via the biosphere by net primary production is 62.7 Terawatts (TW). They suggested that approximately 1 TW of the energy produced by net primary production was transferred as

mechanical energy for mixing. This is comparable to both the wind and tidal inputs, which contribute approximately 1 TW each (Wunsch and Ferrari, 2004). Huntley and Zhou (2004) also estimated the turbulent dissipation rates of large aggregations of marine animals. The marine mammals ranged in size from small krill to whales. They concluded that regardless of the size of the marine animal, the turbulent energy rates produced were between 10^{-5} to 10^{-4} W kg⁻¹. In comparison, winds in the upper 10 m at speeds between 5 m s⁻¹ to 20 m s⁻¹ produce turbulent dissipation rates ranging from 10^{-7} W kg⁻¹ to 10^{-6} W kg⁻¹ (MacKenzie and Leggett, 1993). Thus the biosphere is plausibly as important of an energy source as the winds and tides for mixing.

Recent studies have been conducted using microstructure profilers to study biologically generated turbulence. These studies focused mainly on diel vertical migrations of krill and aggregations of nekton in coastal inlets and bays in the upper 200 m. Kunze *et al.* (2006) observed the DVM of krill in Saanich Inlet, British Columbia using an echosounder to track the biomass through the water column and a tethered microstructure profiler to collect coincident dissipation rates. They observed enhanced turbulent dissipation levels within the detected biomass layer during the DVM between 10^{-5} W kg⁻¹ to 10^{-4} W kg⁻¹, three to four orders of magnitude above background levels. Gregg and Horne (2009) used similar methods to that of Kunze *et al.* (2006) within an aggregation of nekton, most likely of fish origin, in Monterey Bay. They found turbulent dissipation rates between 10^{-6} W kg⁻¹ to 10^{-5} W kg⁻¹. These observations are consistent with the DSL contributing importantly to turbulent kinetic energy, however connections are tenuous at best. Gregg and Horne (2009) also argued that bio-turbulence did not mix tracers, and Rousseau *et al.* (2010) in a follow up experiment failed to replicate Kunze *et al.* (2006) previous observations of $O(10^{-5}$ W kg⁻¹) in Saanich Inlet. We note these studies were all conducted in the surface ocean.

QUANTIFYING PARAMETERS

1.1 Dissipation

Molecular processes govern the ultimate fate of all the energy in the ocean. Viscous dissipation, ε , represents the action of friction in converting turbulent kinetic energy to heat and occurs at very small scales. This is in turn the end state in a cascade of energy from larger scales, where the winds and tides are presumably dominant. Microstructure profilers measure velocity at micro-resolutions $O(<0.5 \text{ m})$ along a vertical trajectory. These observations can be used to calculate the vertical shear of the velocity, u_z , against small scales. Averaging the shear measurements allow an estimate of dissipation as,

$$\varepsilon = (15/2)\nu \langle u_z^2 \rangle \quad (\text{W/kg}),$$

where $\nu = 10^{-6} \text{ m}^2 \text{ s}^{-1}$ is the molecular viscosity of seawater and $\langle u_z^2 \rangle$ is the mean-square turbulent shear (Osborn, 1980). The fraction, $15/2$, comes from the assumption that at the microstructure level the dissipation fluctuations can be taken to be isotropic (Yamazaki and Osborn, 1990). Thus, the shear components are taken to be equal in all directions, which allows for the dissipation to be measured by just one component. Yamazaki and Osborn (1990) were able to show that using this isotropic relation yields a good estimate of dissipation.

1.2 Shear

The above direct estimate of ε employs small-scale shear. Shear, u_z , at larger scales can be used to determine the dynamical stability of the flow, which is governed by the gradient Richardson number,

$$\text{Ri} = N^2 / (u_z)^2,$$

where N is the Brunt-Vaisala frequency. This represents a competition between

the destabilizing effects of shear and the stabilizing effect of buoyancy. If $Ri < \frac{1}{4}$ then the shear layers may become dynamically unstable and can overturn. Estimates below the critical Ri ($Ri < \frac{1}{4}$) on the scales of 10 m are often related to high ε measurements arguing dynamical instability as the cause of oceanic turbulence.

1.3 Volume Backscattering Strength

The backscattering strength, s_v , is a measure of the concentration of fish in the water column,

$$s_v = N_f \sigma_{bs} \text{ (m}^{-1}\text{)},$$

where N_f is the number of scatterers per unit volume and σ_{bs} is their backscattering cross section. Converting to decibels, we have

$$S_v = 20 \log_{10}(s_v),$$

where S_v is the volume backscattering strength (Clay, S. C. and H. Medwin, 1977). The backscatter is the result of an active pinging of the water column, and the time lag of the signal S_v from the initial ping can be related to the depth of the scatterers.

INSTRUMENTATION

This study uses three instruments to obtain the observations necessary for each parameter. A 50 kHz hydrographic Doppler sonar system (HDSS) was used to determine the velocity vectors. A 38 kHz Simrad EK60 echo sounder was used to resolve the biomass layers. A deep microstructure profiler (DMP) was used to obtain the turbulent dissipation rates. All three of these instruments are capable of reaching depths of at least 1000 m, with the echo sounder and the DMP capable of much greater depths. We now discuss the instruments individually.

1.4 Deep Microstructure Profiler (DMP)

The Deep Microstructure Profiler (DMP) was built by Rockland Scientific International (Figure 2). The DMP is a free falling profiler (i.e. it has no cable attachments once deployed) that measures both microstructure and fine-structure data. Microstructure typically refers to processes on vertical length scales of less than 0.5-m, whereas fine-structure refers to the larger length scales above 0.5-m. This is done by 6 probes that measure shear, temperature and conductivity at resolutions of $O(1)$ mm to $O(1)$ m. In addition, a CTD supplies fine-scale salinity, temperature and pressure measurements at resolutions above $O(1)$ m. The profiler falls at a nominal velocity of 0.65 m/s.

Shear measurements are only made during the descent (during the ascent the shear probes trail the instrument and the turbulent wake would contaminate any observations), while salinity and temperature are recorded roundtrip. At the bottom of the dive two expendable weights are released allowing the profiler to

obtain positive buoyancy and float to the surface¹. The profiler is equipped with a triple redundant weight release system. The DMP has a dissipation rate noise level of $1 \times 10^{-10} \text{ W kg}^{-1}$, due to turbulence created by the nose of the profiler guard and from vibrations of the instruments and electronic noise.

For the fine-structure data, the parameters collected by the DMP's Seabird CTD are conductivity, temperature, and pressure. The microstructure data consists of shear, temperature, and conductivity and are sensed via two independent air-foil shear probes mounted 1-cm apart, an FP07 fast response thermistor, and a dual electrode conductivity cell, respectively (Polzin and Montgomery, 1996). The primary goal in collecting microstructure data is to obtain accurate estimates of the averaged gradient variances (e.g. $\langle u_z^2 \rangle$). To achieve this the profiler samples the microstructure data at 512 Hz resulting in shear data every 0.0033 meters.

1.5 Hydrographic Doppler Sonar System (HDSS)

Shear data was also obtained from velocity measurements using the hull-mounted hydrographic Doppler sonar system (HDSS) aboard the *R/V Roger Revelle*. The HDSS consists of a long-range 50 kHz sonar able to penetrate down to depths of 1000 m. The ability to penetrate to such depths is at a loss to the vertical spatial resolution. The HDSS measures Doppler shift by reflecting an acoustic signal off of particulates and bubbles that are passively flowing with the currents in the water column, in order to determine the direction and speed of those currents. This can limit the depth of coverage depending on the amount of particulates that occupy the water column. Near the surface, this tends to not be a problem, as ample amounts of particulate are supplied by the biology. Below

¹ The profiler is equipped with a triple redundant weight release system, consisting of a pre-programmed fail-safe timer, a pressure sensor release, and a last resort set of magnesium pins that erode after several hours of exposure to salt water.

several hundred meters, the concentration of particulates can decrease drastically, making it more difficult to recover a signal. The 50 kHz sonar returns profiles with a 9-m binned depth resolution.

1.6 Simrad EK60 Echosounder

The prey field measurements are obtained with a Simrad EK60 echosounder deployed at the surface, which samples at 38 kHz. The transducer emits short sound pulses that reflect off targets within the water column (in this case small marine animals), and are then received back by the transducer. The signal is then sorted into 1-m depth intervals. Sampling at such a low frequency decreases the resolution, but allows for the detection of large biomass features to depths of 2000 m.

1.7 Data

Turbulent dissipation profiles are estimated by averaging 50-m depth bins. The average of each bin is calculated along with the 95% confidence intervals estimated using a Monte Carlo bootstrap method. The microstructure data is plotted in reference to typical open ocean background levels of $1 \times 10^{-10} \text{ W kg}^{-1}$. The acoustic backscatter data is represented as both a time series and as profiles consisting of 50-m depth bins, with the standard deviations calculated for the binned profiles. The acoustic backscatter is plotted against a reference of -90 db, which represents a low density of biomass concentration. The shear data is represented as a times series. Each time series and binned profile is comprised of data spanning one hour, roughly the amount of time it takes for each microstructure profile.

OBSERVATIONS

The prey-field mapping cruise took place over a two-week period, between 9/15/2008 and 10/01/2008, in the TOTO within the Bahamas archipelago (Figure 1). Biological and physical measurements were taken off the east coast of Andros Island as a series of “clover” surveys between latitudes 24°N - 25°N and longitudes 77°W - 78°W. The physical parameters that were sampled consisted of temperature, salinity, velocity, shear, and turbulence. The biological measurements consisted of the depths and densities of the biomass layers from the acoustic backscatter intensity. From these measurements, the location and spatial distribution of the biomass layers as well as the associated physical properties in the TOTO region are determined. Thus, we may obtain turbulent dissipation measurements and determine the processes responsible for the generation of enhanced turbulence dissipation.

The six clover surveys consisted of 18 microstructure profiles, 3 in each clover, as well as simultaneous measurements of acoustic backscatter and velocity, from which the shear can be calculated. The profiling strategy consisted primarily of two consecutive profiles taken at the center of each clover with a third taken at the apex of the clover "leaf" (Figure 1). The purpose of the clover track is to capture the spatial variability of the prey and turbulence field over a scale of 6 km and over the course of 6-8 hours. The clovers were taken across the TOTO, ranging in depths from 600 m next to Andros Island to 2000 m in the interior. However, only the upper 800 m is considered for comparison, as this is the depth range where the majority of biological activity is observed. Two of the clovers transect the shelf break on the west coast of Andros Island, with the remaining four clovers taken in the interior region. Three of the clovers were started at dusk in an attempt to capture elevated turbulent dissipation rates associated with the

DVM of nekton out of the deep scattering layer (DSL). The remaining three clovers were conducted during the night post-DVM.

1.8 Clover Survey Results

The backscatter signal detected several biological features during the clover survey (Figures 2,3). At this frequency, features such as the sea floor and seamounts, in excess of 1500-m, are resolved (i.e. Figure 4). The DSL is a constant feature observed throughout the entire clover survey. It typically remains around 500-m, with a vertical thickness of 150-200 m, while in the horizontal it spans the TOTO region where waters are deeper than 1500 m. The volume backscattering strength S_v within the DSL typically ranged between -75 to -70 db in comparison to the background levels of the acoustically quiet waters between -90 to -95 db (i.e. Figure 2, 3).

The DVM is represented by a clear gain in volume backscattering strength throughout the water column above the DSL. The DVM was only detected during the dusk profiles at stations 2, 7, and 10 of clovers 2, 4, and 5 (Figure 2). The migrating layer ranged in thickness from ~100 m in station 7 (Figure 2,4) to spreading the entire water column above the DSL at stations 7 and 10 (i.e. Figure 2,5). The DVM elevated the acoustically quiet background levels above the DSL to S_v ranging from -80 to -70 db. The S_v observed in the SSL ranged from -75 db during the dusk migration period to levels exceeding -70 db during the night (Figure 2). The loss of volume backscattering strength in the DVM is consistent with the vertical orientation of marine animals during migration (Simard and Sourisseau, 2009).

Dissipation rates observed during the clover survey exceeded $10^{-8} \text{ W kg}^{-1}$, two orders of magnitude above background levels, in 9 out of the 18 profiles

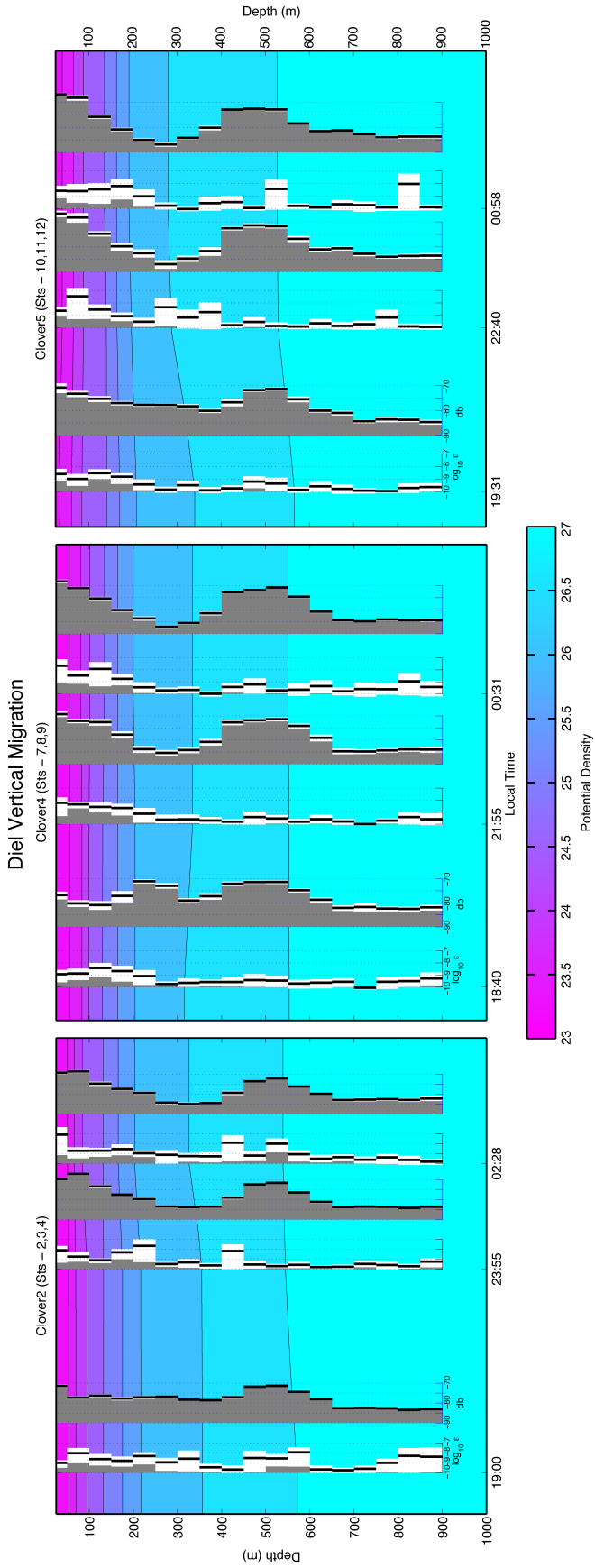


Figure 2. Plot of clovers 2, 4, and 5 conducted during the DVM comparing the dissipation rates to the volume backscattering strength with the potential density contours in the background. The profile to the left is the dissipation profile with the bold vertical line representing the mean bin values and the white area the 95% confidence intervals. A logarithmic axis is used for the dissipation data plotted about a reference level of $\epsilon = 1 \times 10^{-10} \text{ W kg}^{-1}$, corresponding to the background dissipation level. The acoustic data is plotted with a reference level of -90 db.

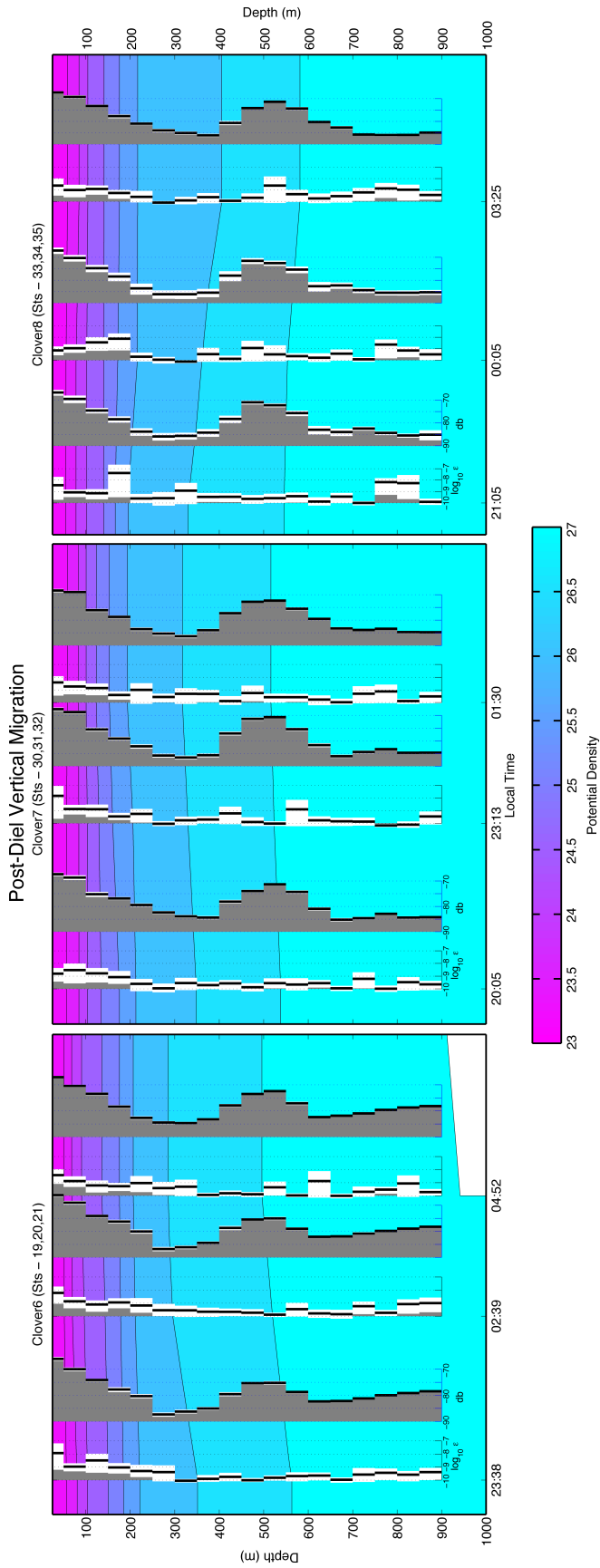


Figure 3. Plot of clovers 6, 7, and 8 conducted post-DVM comparing the dissipation rates to the volume backscattering strength with the potential density contours in the background. The profile to the left is the dissipation profile with the acoustic profile to the right in each pair of profiles. The data is estimated over 50 m depth intervals with the bold vertical line representing the mean bin values and the white area the 95% confidence intervals. A logarithmic axis is used for the dissipation data plotted about a reference level of $\epsilon = 1 \times 10^{-10} \text{ W kg}^{-1}$, corresponding to the background dissipation level. The acoustic data is plotted with a reference level of -90 db.

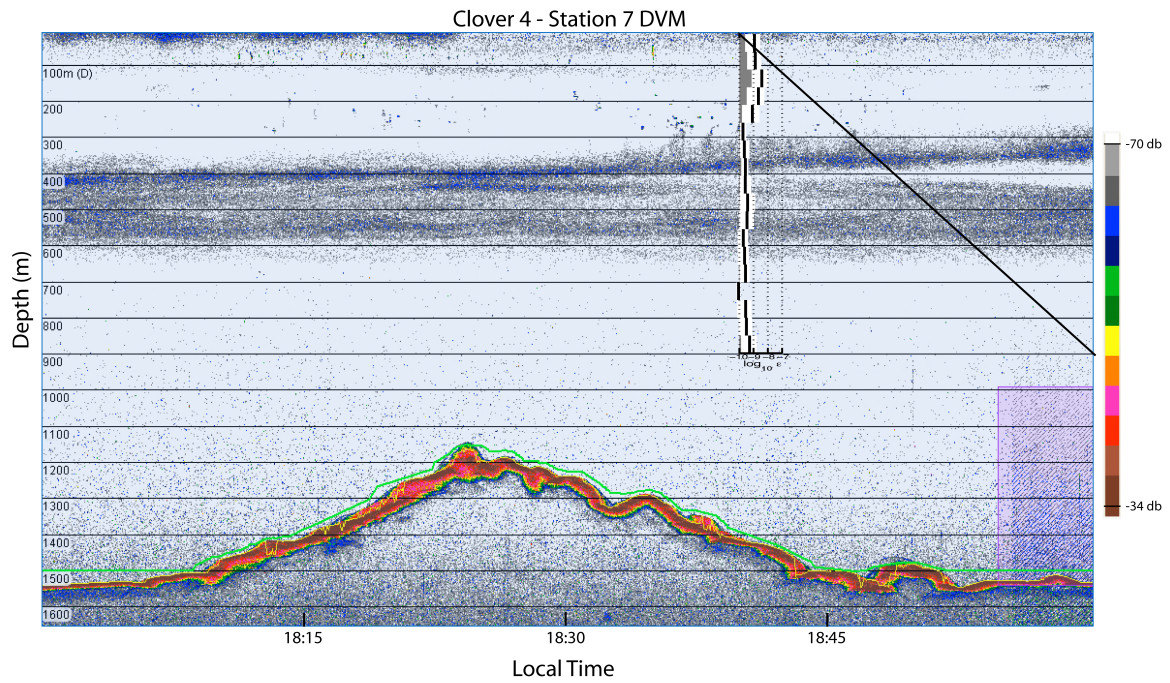


Figure 4. Station 7 from clover 4 plotted on top of the volume backscattering strength time series. The slanted bold line represents the estimated location of the profile through the water column with time.

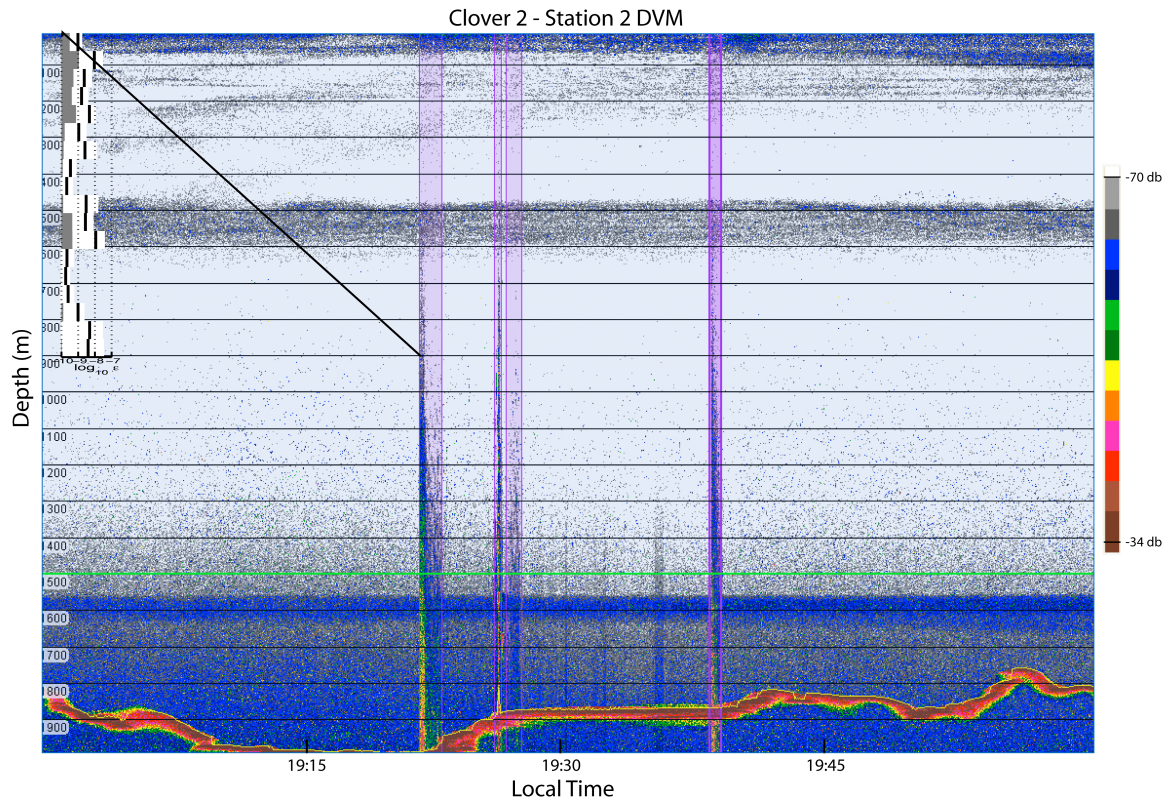


Figure 5. Station 2 from clover 2 plotted on top of the volume backscattering strength time series. The slanted bold line represents the estimated location of the profile through the water column with time.

(Figures 2 and 3). The majority of elevated dissipation rates were within the biomass layers, however, there were elevated dissipation rates within the acoustically quiet waters suggesting turbulence production in the TOTO region may originate from other sources (i.e. shear, internal waves). In the DSL dissipation rates exceeded $10^{-9} \text{ W kg}^{-1}$ in 7 out of the 18 profiles. Sustained dissipation rates were observed in the SSL between 10^{-9} to $10^{-8} \text{ W kg}^{-1}$ in the top 300 m in most of the profiles (Figure 2). The three stations, 2, 7, and 10, during the DVM also recorded dissipation rates between 10^{-9} to $10^{-8} \text{ W kg}^{-1}$.

The shear generated in the TOTO region was predominantly constrained to the surface layer extending down to 200 m (Figures 6-9). Below the surface the region was relatively quiet in terms of shear production, specifically between 400-600 m where the DSL resides. There is a common trend within the main biomass layer, where three cases exist; 1) elevated dissipation signals with minimal shear (Figure 6), 2) moderate shear with no elevated dissipation rates (Figure 7), or 3) no signal in shear or dissipation rates (Figure 9). Case 1 occurred most frequently in 6 of the 15 stations (i.e. Figure 6)². The first stations in clovers 4 and 8 are consistent with case 2, which was observed in 3 of the 15 stations (i.e. Figures 7 and 8). Case three occurred in 5 of the 15 profiles and is observed in the first and last stations of clover 7 (Figure 9).

1.9 Clover Survey Discussion

There were no bursts of dissipation rates of $O(10^{-5} \text{ W kg}^{-1})$ during the DVM like those observed by Kunze *et al.* (2006). The profile of station 2 (and similarly station 10) passed through a low density biomass layer, which may account for the low dissipation levels observed (Figure 5). However, in Figure 4 the profile at

² Clover 6 did not collect velocity data during the DMP profile for the shear comparison.

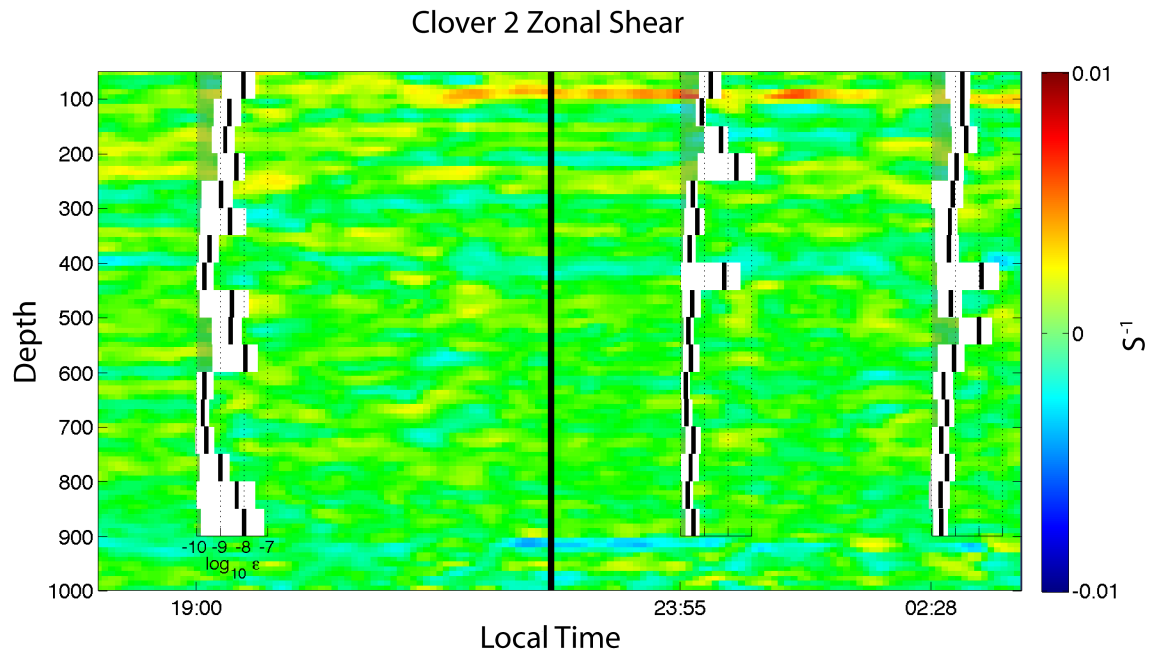


Figure 6. Plot of the Clover 2 survey comparing the dissipation profiles plotted on top of the zonal shear. For reference the deep scattering layer (DSL) resides approximately between 400 to 600 m.

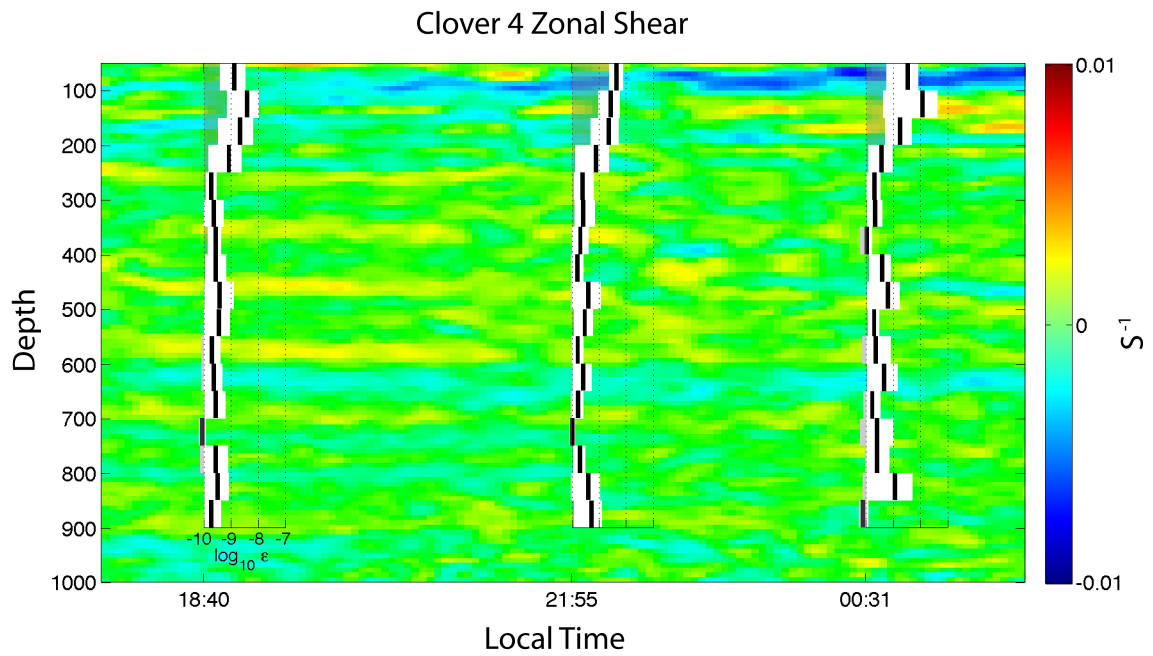


Figure 7. Plot of the Clover 4 survey comparing the dissipation profiles plotted on top of the zonal shear. For reference the deep scattering layer (DSL) resides approximately between 400 to 600 m.

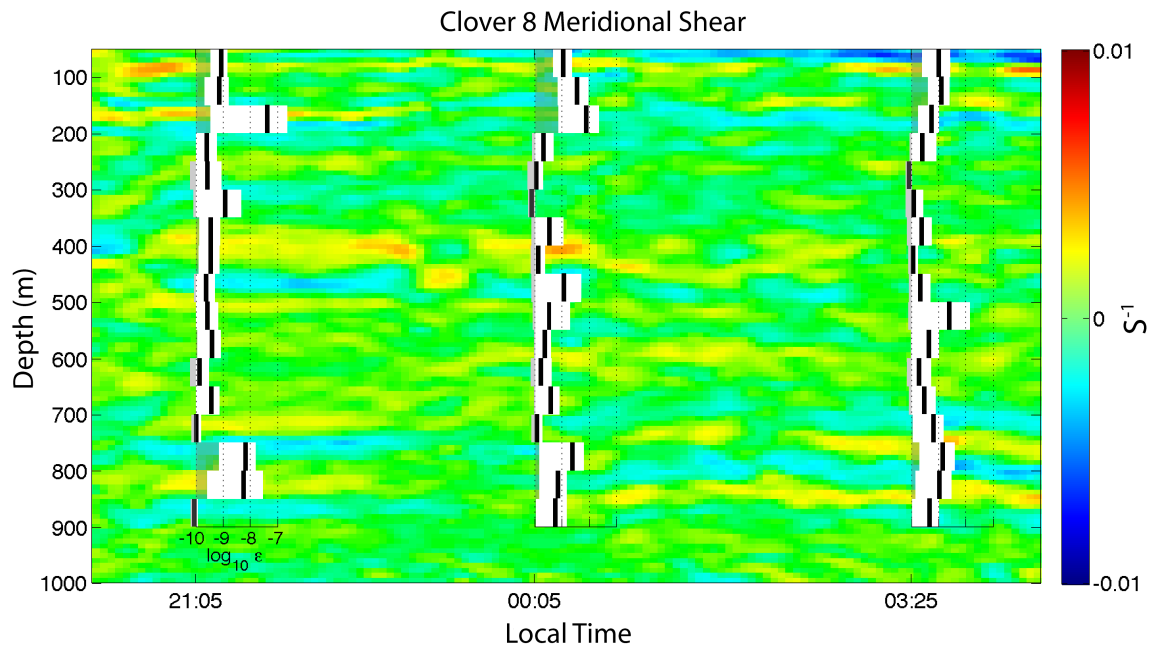


Figure 8. Plot of the Clover 8 survey comparing the dissipation profiles plotted on top of the meridional shear. For reference the deep scattering layer (DSL) resides approximately between 400 to 600 m.

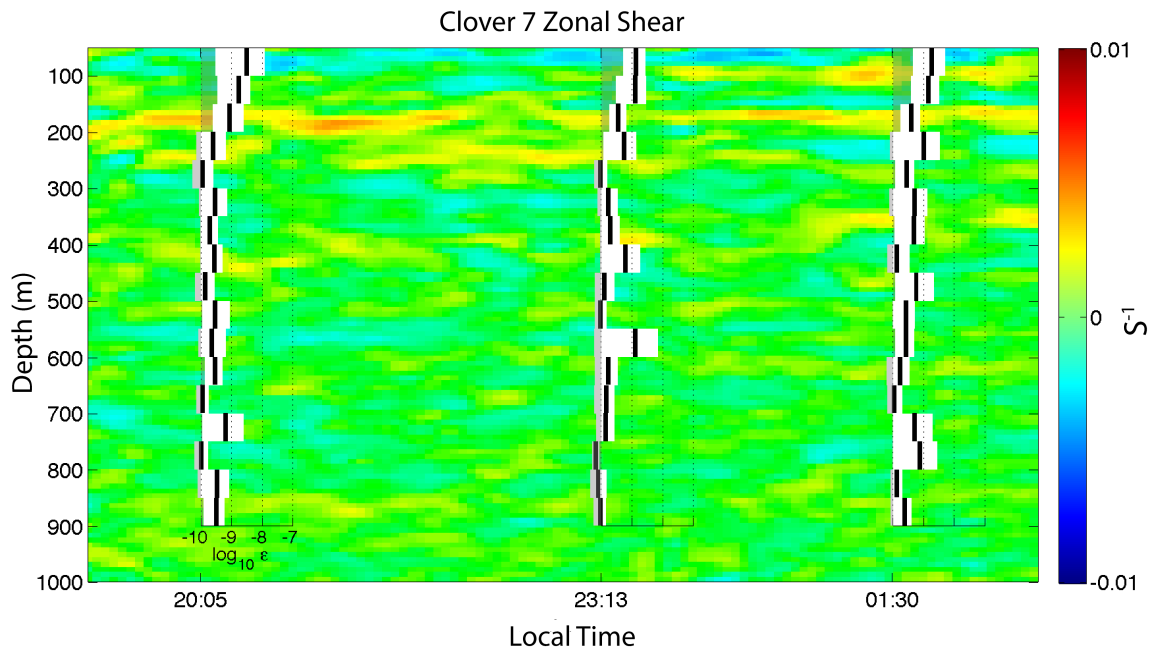


Figure 9. Plot of the Clover 7 survey comparing the dissipation profiles plotted on top of the zonal shear. For reference the deep scattering layer (DSL) resides approximately between 400 to 600 m.

station 7 passed through a well-established 100-m thick biomass layer during its vertical ascent where dissipation rates observed were of $O(10^{-10} \text{ W kg}^{-1})$. This is consistent with the observations of Rouseau *et al.* (2010) and Rippeth *et al.* (2007) who failed to observe elevated dissipation rates during vertical migration events comparable to Kunze *et al.* (2006).

Within the DSL, minimal turbulent dissipation rates were observed, typical of background levels found in the abyssal open ocean away from complex topography. However, there are signs of moderate elevated patches within the DSL between 10^{-9} to $10^{-8} \text{ W kg}^{-1}$ scattered amongst the profiles (Figure 2,3). Clover 2 demonstrates the most activity amongst the clovers within the DSL, with moderate elevated dissipation rates observed in all three stations between $(0.66 - 1.2) \times 10^{-8} \text{ W kg}^{-1}$ (Figure 2). The rest of the profiles have observed dissipation rates comparable to background levels between $(1 - 36) \times 10^{-10} \text{ W kg}^{-1}$ (Figure 2,3). Dissipation rates within the DSL are several orders of magnitude lower than predicted by Huntley and Zhou (2004) and those observed by Gregg and Horne (2009) in large aggregations of nekton. Hays *et al.* (2010) proposed that the DSL is a sanctuary from predation where prey remain at depth fasting until energy reserves become depleted forcing them to migrate to the surface under the protection of night to feed. This likely explains the lack of energetic local motion within the DSL resulting in low observations of turbulent dissipation rates.

The SSL can be seen at the surface, above 200 m, in all the clovers, omitting the first stations in the three clovers that began during dusk (Figures 2 and 3). The dissipation rates are comparable to those seen in the DSL and DVM, with the majority of dissipation rates remaining below $10^{-9} \text{ W kg}^{-1}$. However, there are several patches of dissipation rates near or exceeding $10^{-8} \text{ W kg}^{-1}$ observed in the clover profiles. It is difficult to determine the cause of the raised dissipation rates near the surface, resulting from the influence of turbulence generated by surface processes.

From the velocity, temperature, and salinity profiles, the shear, u_z , and the gradient Richardson number, $Ri = N^2/(u_z)^2$, was calculated to assess the dynamic stability within the biomass layers. The Ri numbers for clovers 2 and 8 can be seen in Figures 10 and 11, which are representative of the TOTO region. The critical value, $Ri = 0.25$, is represented by the blue vertical line; values less than 0.25 argue for shear instabilities where elevated dissipation rates can be expected. In Figures 9 and 10 values below the critical Ri number are observed mainly outside of the DSL. This suggests, further, that the DSL (approx. between 400-600 m) is a dynamically stable region where the generation of intense turbulence associated with mixing is not likely to occur. However, the Ri number only establishes where areas may become dynamically unstable, which is often associated with larger dissipation rates. This does not, however, rule out the possibility of shear as the generator of the low dissipation rates observed.

The correlation coefficients were calculated between the dissipation rates and the volume backscattering strength and between the dissipation rates and the shear (Figure 12,13). The depth interval from 300-900 m was chosen to eliminate the surface influences where multiple processes, such as winds, waves and biology, may all be contributing to turbulence production. The 95% confidence intervals were calculated using a bootstrap method. Anything above the horizontal blue dotted line represents moderate to strong correlations.

The dissipation rates are overall poorly correlated with the volume backscattering strength and the local shear. However, the dissipation rates in stations 2 and 4 show strong correlation coefficients to the volume backscattering strength of $r = 0.66$ and $r = .71$, respectively (Figure 6). The correlation values suggest that the events are not random, from which one could argue that the biology may be responsible for the turbulence. The shear does show some strong correlation with the dissipation rates in stations 33, 34, and 35 with correlation coefficients of $r = .76$, $r = .57$, and $r = .72$, respectively (Figure 8). The high correlations, again,

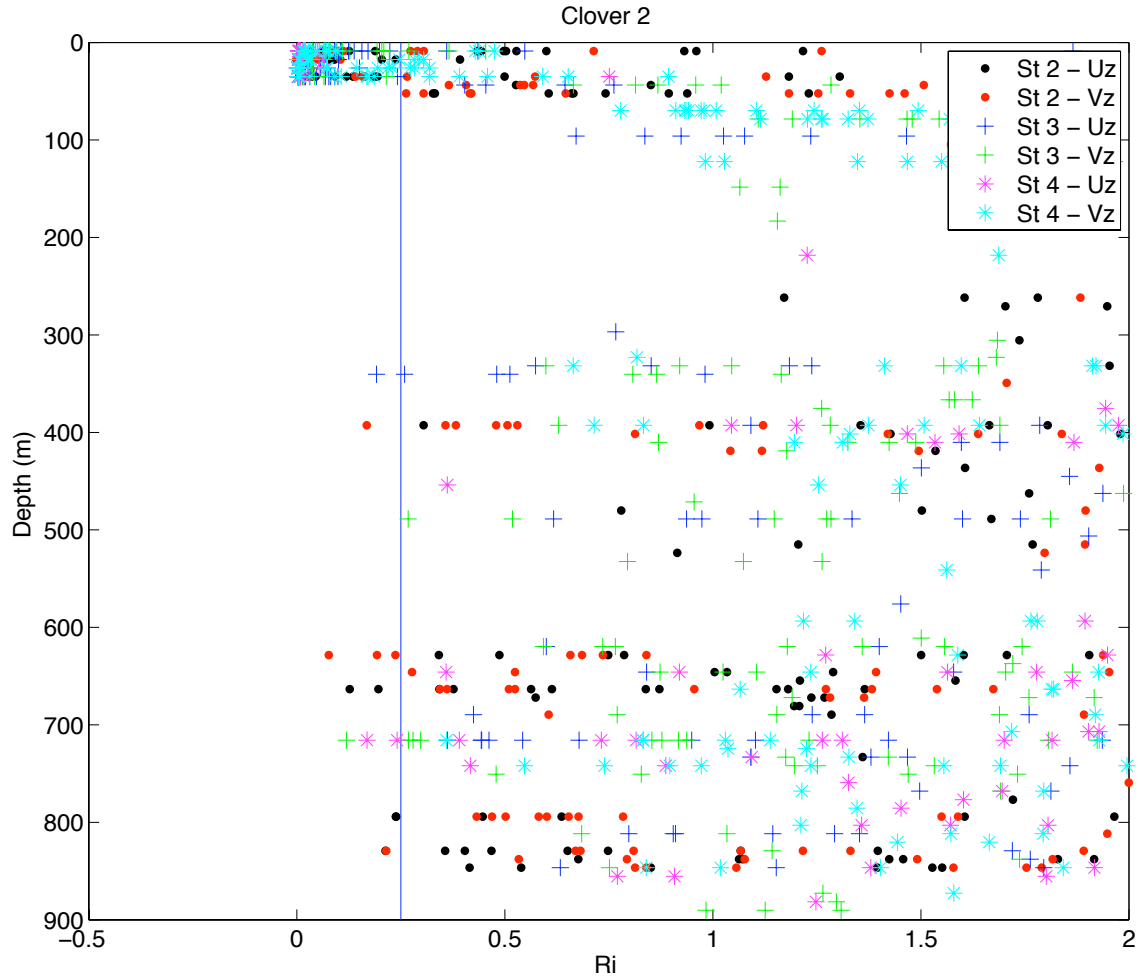


Figure 10. Gradient Richardson number (Ri) for Clover 2. The vertical blue line represents the critical Ri number, $Ri < 0.25$.

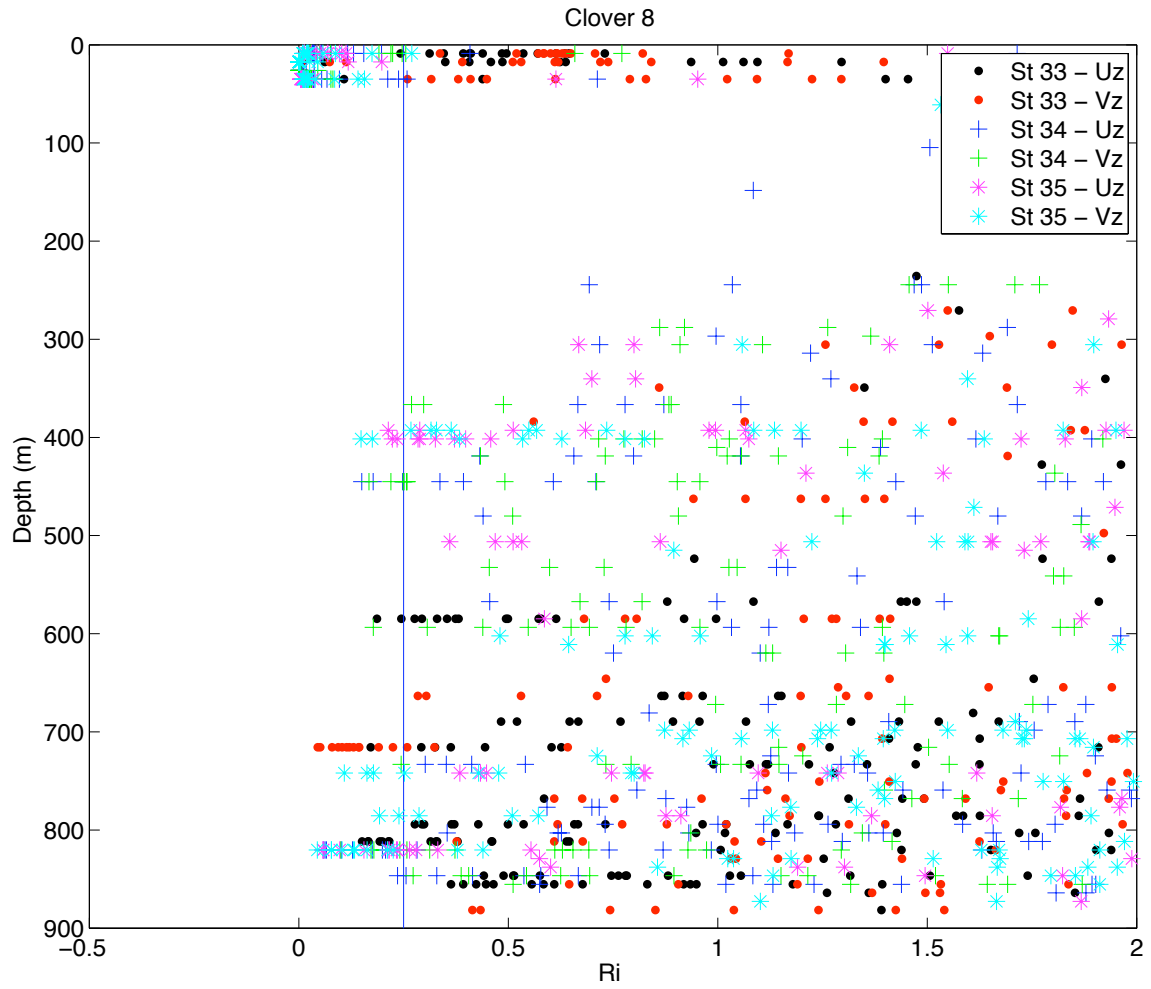


Figure 11. Gradient Richardson number (Ri) for Clover 8. The vertical blue line represents the critical Ri number, $Ri < 0.25$.

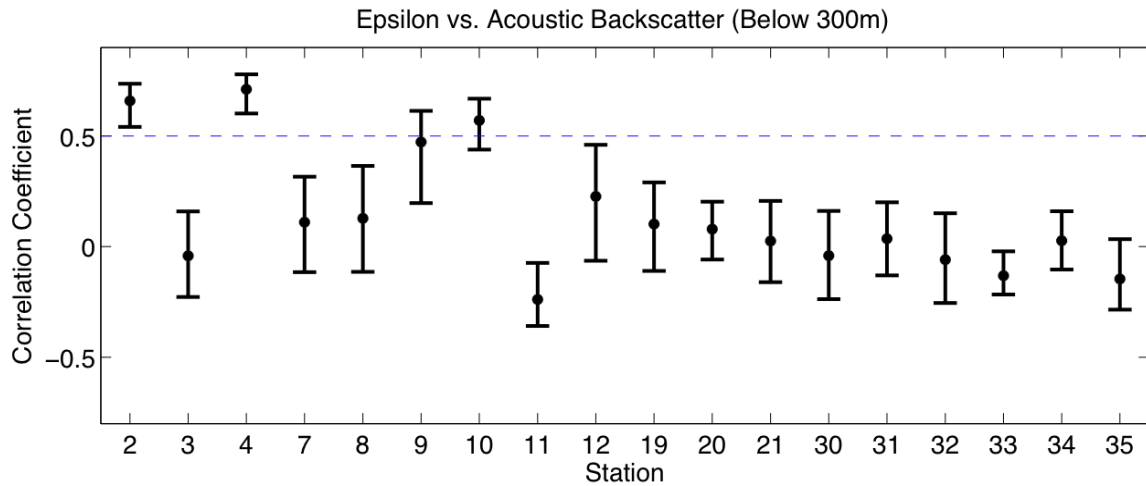


Figure 12. Correlation coefficients between dissipation rates and volume backscattering strength representing profiles below 300 m to eliminate surface signals. The horizontal bars with each dot represents the 95% confidence interval. The blue dotted line at 0.5 represents moderate or better correlations.

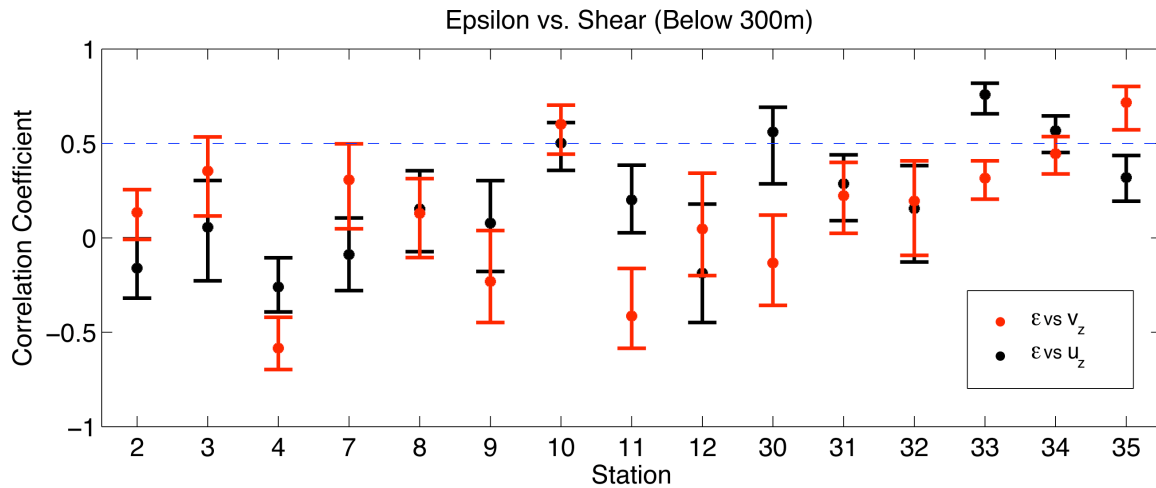


Figure 13. Correlation coefficients between epsilon and zonal (black) and meridional (red) shear representing profiles below 300 m to eliminate surface signals. The horizontal bars with each dot represents the 95% confidence interval. The blue dotted line at 0.5 represents moderate or better correlations.

suggest that these events did not occur randomly indicating that the shear may be responsible for some of the turbulence within the DSL. However, the shear correlated to the elevated dissipation levels appears to be mainly with the middle station, 34.

1.10 Inter-Site Comparison

The dissipation rates from the clover survey are compared to those of the North Atlantic Tracer Release Experiment (Figure 14). The North Atlantic Tracer Release Experiment (NATRE) survey was conducted in the Canary Basin in 1992 from March to April. The High Resolution Profiler (HRP) was used to measure the microstructure data, the details of which are described by Schmitt *et al.* (1988). The survey consisted of 150 HRP profiles down to an approximate depth of 2000-m in a water depth of roughly 4000 m. Of the 150 profiles, 10 were done to 3000 m in a water depth of approximately 5500 m. The clover survey consisted of 18 DMP profiles. The depth ranged from approximately 1000 m near the walls of the trough to approximately 1800 m in the interior.

The ensemble averages of the stations from each site were used (Figure 15). The profiles are averaged over 50-m bins using a bootstrap method to obtain the confidence intervals. The bold vertical line represents the average value of each bin with the lighter shading representing the 95% confidence intervals.

The NATRE location was chosen to study the turbulence of the deep ocean in the absence of sources of internal wave energy from complex topography. As a result the NATRE data has come to represent the typical observation of the background ocean turbulence state. The TOTO data appears to agree relatively well, representing typical background levels for the region. There are three

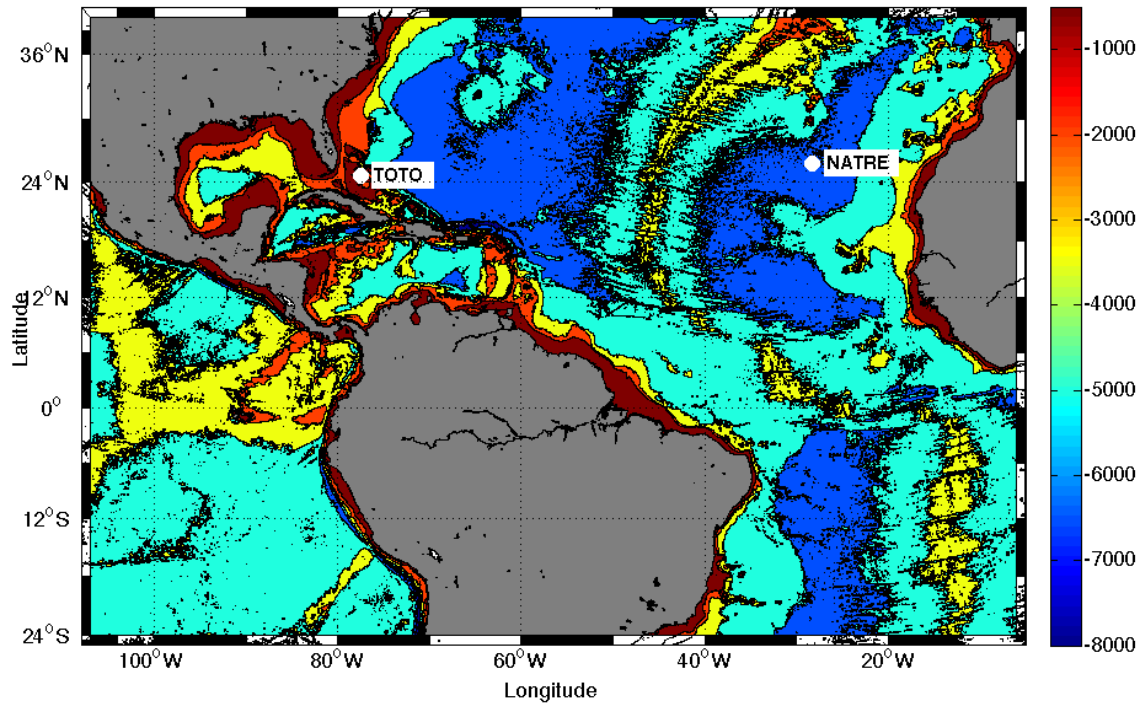


Figure 14. Site map of the TOTO and NATRE locations.

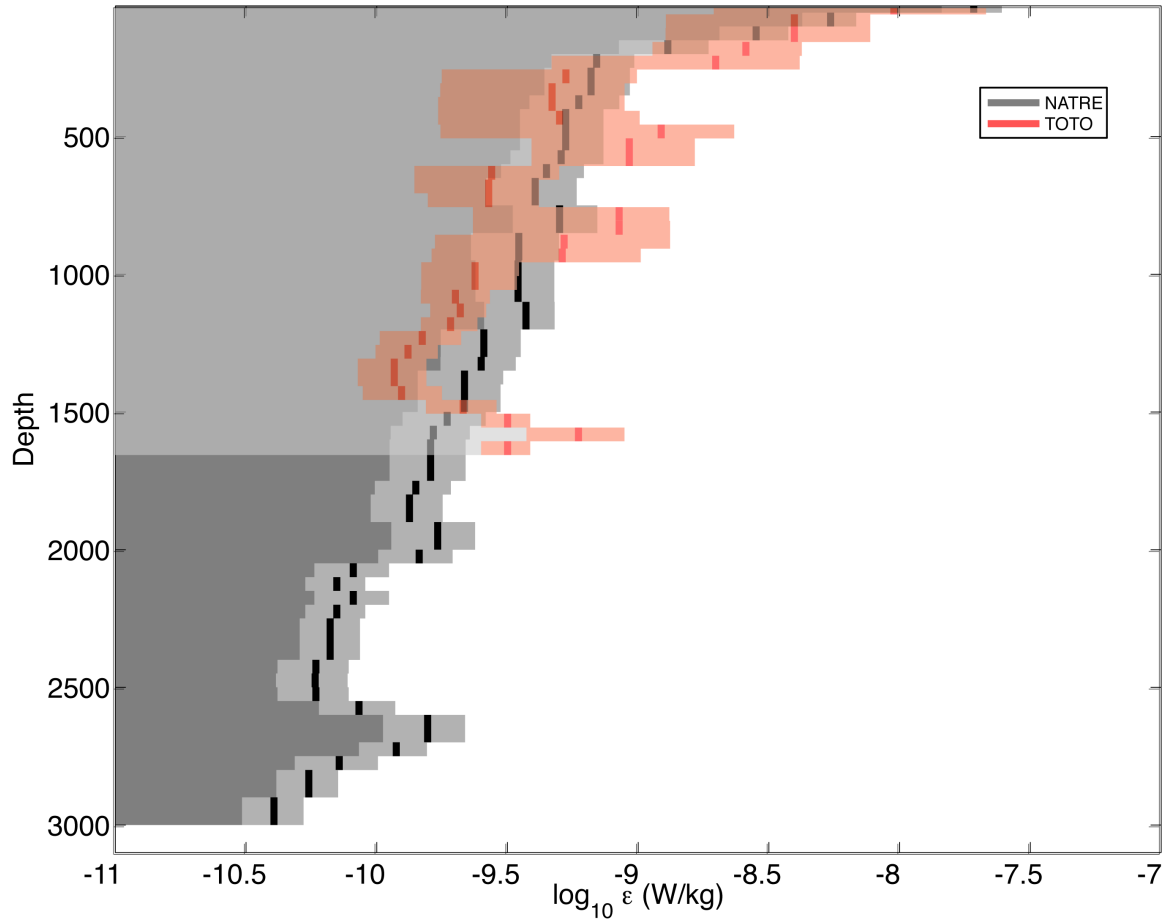


Figure 15. Ensemble average profiles of turbulent dissipation rate estimated from microstructure measurements at two different deep ocean sites. Depth bins of 50 m were used in calculations of the 95% confidence interval (colored bands) and mean (bold vertical lines inside each band).

modest enhancements of dissipation seen at approximately 600 m, 800 m, and 1700 m. The enhanced dissipation seen at 600 m most likely represents the dissipation rates observed within the DSL located between 400-600 m. The enhancement seen at 800 m are possibly a response to shear instabilities seen in the Richardson number calculations (i.e. Figure 11). The dissipation rates seen in the clover survey at 1700 m are likely due to elevated dissipation rates due to bottom processes. Although the TOTO site is comparatively a much more complex region than the NATRE site, the shelter provided by the island archipelago appears to protect the area from being a source of enhanced turbulence.

CONCLUSION

The prey-field mapping cruise of the TOTO region suggests a large biomass layer between 400-600 m throughout the entire region associated with low to moderate patchy turbulence. The Rothschild-Osborn hypothesis was examined, which suggests that zooplankton seek areas of elevated turbulence. If this were the case for the DSL then one would expect the coincidence of physical processes responsible for generating turbulence, such as shear, and elevated biomass to be more frequent. However, this was not the case for most of the profiles in the DSL. Stable dynamical conditions were observed in areas of deep biomass layers, such as the DSL (Figures 6). Alternatively, areas with moderate shear and marginally unstable conditions within the biomass layer, such as clover 4, lacked associated observations of elevated dissipation rates (Figure 7). Furthermore, the Ri numbers showed very little evidence to support a dynamically unstable region within the DSL. This suggests that the shear is not responsible for the patches of turbulence detected within the DSL. Furthermore, this suggests that the location of the DSL is not dependent on the turbulence levels. In clover 8 there appeared to be shear instabilities correlated with moderate dissipation levels. However, with there being the only incident in the clover survey, station 34, it seems unlikely that the location of the DSL is dependent on turbulence levels. However, it is not clear that the Rothschild-Osborn hypothesis should apply to the DSL, where the biomass of interest were nekton and hunting activities may be limited.

Overall, the analysis of the region does not seem to support either the biology or the shear as a dominant process driving the moderate turbulence observed. The correlation coefficients for clover 2 suggested that the biology was responsible, while clover 8 presented an argument for shear as the possible force. The

gradient Richardson number suggests that the DSL is a dynamically stable region. This does not, however, eliminate the capability of shear to generate the low levels of turbulence observed. The results suggest that a combination of the biomass layers and the shear are responsible for the observed elevated turbulence dissipation rates. However, dissipation rates were never observed in excess of $O(10^{-8} \text{ W kg}^{-1})$ as compared to dissipation rates of $O(>10^{-5} \text{ W kg}^{-1})$ observed in other areas of complex topography (Lueck and Mudge, 1997, St. Laurent and Thurnherr, 2007) and in large nekton aggregations (Gregg and Horne, 2009, Kunze *et al.*, 2006). The results are consistent with the DSL as a safe haven from predators (Hays *et al.*, 2010), where nekton most likely conserve their energy reserves until migrations to the surface take place.

The results of the comparison with the data from the NATRE site suggest that the TOTO region is relatively quiet in terms of turbulence production. With average dissipation rates on the order of $(1-10 \times 10^{-10} \text{ W kg}^{-1})$ the complex topography of the TOTO region does not seem to play a significant role of turbulence generation.

REFERENCES

- Brekhovskikh, L. M. and Y. P. Lysanov (2003). *Fundamentals of Ocean Acoustics*. New York, NY: AIP Press.
- Clay, S. C. and H. Medwin (1977). *Acoustical Oceanography: Principles and Applications*. New York, NY: John Wiley & Sons.
- Dewar, W.K., R. J. Bingham, R. L. Iverson, D. P. Nowacek, L. C. St. Laurent and P. H. Wiebe (2006), Does the marine biosphere mix the ocean?, *J. Mar. Res.*, 64, 541-561.
- Gregg, M. C. and J. K. Horne (2009) Turbulence, acoustic backscatter, and pelagic nekton in Monterey Bay, *Amer. Met. Soc.*, 39, 1097-1114.
- Hays, G. C. (2003), A review of the adaptive significance and ecosystem consequences of zooplankton diel vertical migrations, *Hydrobiologia*, 503, 163-170.
- Hays, G. C., H. Kennedy, B. W. Frost (2010), Individual variability in diel vertical migration of a marine copepod: Why some individuals remain at depth when others migrate, *Limnol. Oceanogr.*, 46, 8, 2050-2054.
- Huntley, M. E. and M. Zhou (2004), Influence of animals on turbulence in the sea, *Mar. Ecol. Prog. Ser.*, 273, 65-79.
- Kunze, E., J. F. Dower, I. Beveridge, R. Dewey, and K. P. Bartlett (2006), Observations of biologically generated turbulence in a coastal inlet, *Science*, 313, 1768-1770.
- Ledwell, J. R., A. J. Watson and C. S. Law (1993), Evidence for slow mixing across the pycnocline from an open-ocean tracer-release experiment, *Nature*, 364, 701-703.
- Ledwell, J. R., E. T. Montgomery, K. L. Polzin, L. C. St. Laurent, R. W. Schmitt and J. M. Toole (2000), Evidence for enhanced mixing over rough topography in the abyssal ocean, *Nature*, 403, 179-182.
- Lueck, R. G. and T. D. Mudge (1997), Topographically induced mixing around a shallow seamount, *Science*, 276, 1831-1833.

- MacKenzie, B. R. and W. C. Leggett (1993), Wind-based models for estimating the dissipation rates of turbulence energy in aquatic environments: empirical comparisons, *Mar. Ecol. Prog. Ser.*, 94, 207-216.
- MacLeod, C. D., N. Hauser and H. Peckham (2004), Diversity, relative density and structure of the cetacean community in summer months east of Great Abaco, Bahamas, *J. Mar. Biol. Ass. U. K.*, 84, 469-474.
- Mann, D. A. and S. M. Jarvis (2004), Potential sound production by a deep-sea fish, *J. Acoust. Soc. Am.*, 115, 5, 1.
- Munk, W. H. (1966), Abyssal recipes, *Deep-Sea Res.*, 13, 707-730.
- Polzin, K. L., J. M. Toole, J. R. Ledwell, and R. W. Schmitt (1997), Spatial variability of turbulent mixing in the Abyssal Ocean, *Science*, 276, 93-96.
- Rippeth, T. P., J. C. Gascoigne, J. A., M. Green, M. E. Inall, M. R. Palmer, J. H. Simpson, and P. J. Wiles, 2007, Turbulent dissipation of coastal seas. *Science*, [Available online at http://www.sciencemag.org/content/313/5794/768/reply#sci_el_10043?sid=b7700347-db8b-464f-94d3-8b57b447de12.]
- Rothschild, B.J. and T. R. Osborn (1988), Small-scale turbulence and plankton contact rates, *J. Plankton Res.*, 10, 3, 465-474.
- Rousseau, S., E. Kunze, R. Dewey, K. Bartlett, and J. Dower (2010), On turbulence production by swimming marine organisms in the open ocean and coastal waters, *Amer. Met. Soc.*, 40, 2107-2121.
- Schmitt, R. W., J. M. Toole, R. L. Koehler, E. C. Mellinger, and K. W. Doherty (1988), The development of a fine- and microstructure profiler, *J. Atmos. Ocean. Tech.*, 5, 484-500.
- Schwab, W.C., E. Uchupi, R. D. Ballard, and T.K. Dettweiler (1989), Sea-floor observations in the tongue of the ocean, Bahamas: An Argo/SeaMARC survey, *Geo-Marine Lett.*, 9, 171-178.
- St. Laurent, L.C., A. M. Thurnherr (2007), Intense mixing of lower thermocline water on the crest of the Mid-Atlantic Ridge, *Nature*, 448, 680-683.
- Toole, J. M., K. L. Polzin, R. W. Schmitt (1994), Estimates of diapycnal mixing in the abyssal ocean, *Science*, 264, 1120-1123.

Wunsch, C. and R. Ferrari (2004), Vertical mixing, energy, and the general circulation of the oceans, *Annu. Rev. Fluid Mech.*, 36, 281-314.

Yamazaki, H. and T. Osborn (1990), Dissipation estimates for stratified turbulence, *J. Geophys. Res.*, 95, C6, 9739-9744.

BIOGRAPHICAL SKETCH

In the fall of 2005, James A. Hooper V received his Bachelors degree in physics from The Florida State University in Tallahassee, FL. After that he worked as a water quality scientist for the Escambia County Water Quality Division. In the fall of 2007, James enrolled in the masters program in physical oceanography at The Florida State University, where he was advised by Drs. Louis St. Laurent and William K. Dewar. James's research interests include turbulence, upper ocean processes, and biological and physical interactions.